Coronal Loops Workshop VII

Efficient Modeling of Two-fluid Coronal Plasma: Effects of Electron and Ion Heating on Emission Measure

Will T. Barnes & Stephen J. Bradshaw

Department of Physics and Astronomy, Rice University

RICE

Introduction

- Nanoflare model of Parker [8] characterized by energy release on short timescales (e.g. < 200 s)
- Single-fluid models tacitly assume electron and ion populations in equilibrium $\rightarrow$ violated if heating time scale is less than the equilibration (collisional) timescale between the two species
- Two-fluid models often assume that electrons are heated, though ion heating mechanisms have been proposed [see 7]
- Hydrodynamic simulations and forward-modeling allow for calculations of observables that provide signatures of different heating mechanisms
- We have adapted the enthalpy-based thermal evolution of loops (EBTEL) model of Klimchuk et al. [6], Cargill et al. [3, 4] to calculate the temperature and pressure evolution of the electron and ion populations separately while assuming quasi-neutrality (i.e. $n_e = n_i = n$)
- **Goal:** Identify differing observational signatures of electron-versus-ion heating for varying heating frequency through efficient hydrodynamic simulations

Two-fluid EBTEL Model

- Make the following assumptions as outlined in Klimchuk et al. [6], Cargill et al. [3]:
  1. Bulk flow is subsonic $\rightarrow$ neglect terms $\mathscr{O}(v^2)$
  2. Loop is shorter than a gravitational scale height ($z < H_g$) $\rightarrow$ neglect gravitational terms
  3. Transition region length $\ell \ll L$, the coronal loop half-length $\rightarrow$ neglect terms $\mathscr{O}(\ell)$
  4. Semi-circular loop symmetric about the apex
  5. $c_2 = \bar{T}/T_a$ and $c_3 = T_0/T_a$ are constant and independent of species.
  6. Equations closed by ideal gas law for both species $\rightarrow p_e = k_B n T_e,\ p_i = k_B n T_i$
- Applying these assumptions to the field-aligned two-fluid hydrodynamic equations and integrating over the coronal and transition region portions of the loop, we derive two-fluid, time-dependent, spatially-averaged equations for $n,\ T_e,\ T_i,\ p_e,\ p_i$,

$$\frac{d}{dt}\bar{n} = \frac{c_2(\gamma-1)}{c_3\gamma L k_B \bar{T}_e}(\psi_{TR} - F^{(0)}_{c,e} - \mathscr{R}_{TR}), \tag{1}$$

$$\frac{d}{dt}\bar{p}_e = \frac{\gamma-1}{L}[\psi_{TR} + \psi_C - (\mathscr{R}_{TR} + \mathscr{R}_C)] + k_B\bar{n}\nu_{ei}(\bar{T}_i - \bar{T}_e) + (\gamma-1)\bar{E}_{H,e}, \tag{2}$$

$$\frac{d}{dt}\bar{p}_i = -\frac{\gamma-1}{L}(\psi_{TR} + \psi_C) + k_B\bar{n}\nu_{ei}(\bar{T}_e - \bar{T}_i) + (\gamma-1)\bar{E}_{H,i}, \tag{3}$$

$$\frac{d\bar{T}_{e,i}}{dt} = \bar{T}_{e,i}\left(\frac{1}{\bar{P}_{e,i}}\frac{d\bar{P}_{e,i}}{dt} - \frac{1}{\bar{n}}\frac{d\bar{n}}{dt}\right), \tag{4}$$

where

$$\psi_{TR} = \int_{TR} \mathrm{d}s\ v\frac{d}{ds}p_e \approx \frac{1}{1+\xi}(F^{(0)}_{c,e} + \mathscr{R}_{TR} - \xi F^{(0)}_{c,i}), \quad \psi_C = \int_C \mathrm{d}s\ v\frac{d}{ds}p_e \approx \bar{v}p_e^{(a)} - (p_e v)_0, \quad \xi = \frac{T_e^{(0)}}{T_i^{(0)}}.$$

Benchmarking with 1D Hydrodynamic Models

- Field-aligned hydrodynamic code HYDRAD [9] used to benchmark two-fluid EBTEL model
- 0D models such as EBTEL allow for large parameter-space explorations while also capturing (most of) the complex physics of dynamic coronal loops
- Good agreement with 1D model despite HYDRAD incorporating a lot more physics (e.g. shocks, flows, non-equilibrium ionization)

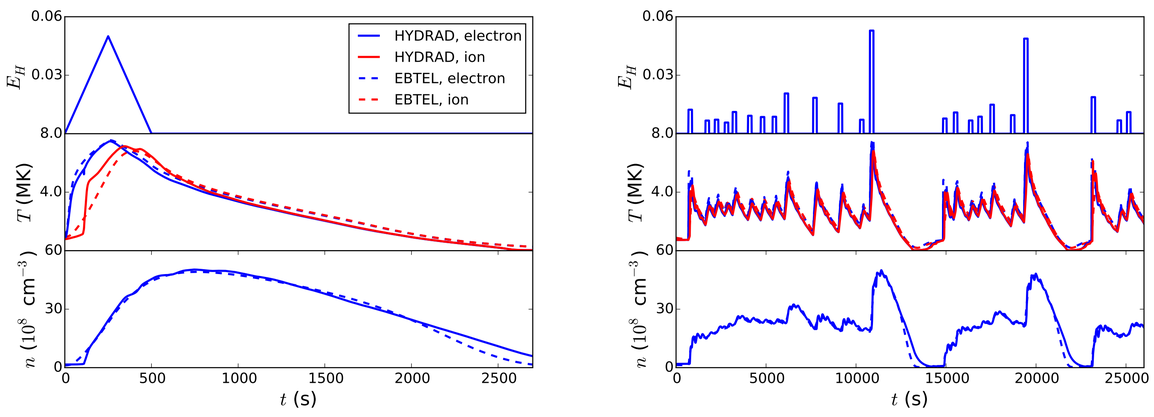

(a) (b)

Figure 1: 1(a) Comparison between two-fluid EBTEL model and HYDRAD for loop with half-length 25 Mm. EBTEL T and n profiles are apex quantities due to averaging in HYDRAD profiles. Heating is triangular pulse lasting 500 s with amplitude 0.05 erg cm^{-3} s^{-1}. 1(b) Same as Fig. 1(a), but for a series of 23 square pulses, each lasting 200 s with amplitudes chosen from a power-law distribution. E_H is in units of erg cm^{-3} s^{-1}.

Heating Function

- Amplitudes either uniform or chosen from power-law distribution
- Power-law runs are constructed such that total number of events is representative of index α independent of heating frequency (see Fig. 2(a))
- Amplitudes are chosen such that for each run, time-averaged heating rate H_n is sufficient to keep a loop in hydrostatic equilibrium at a temperature of ~ 4 MK, consistent with observations [10, 11].
- Heating applied to electron (ion) species through E_H term in Eq. 2 (3)
- Vary heating frequency such that $250 \leq T_N \leq 5000$ s in increments of 250 s, where T_N is the time between consecutive heating events (see Fig. 2(b))

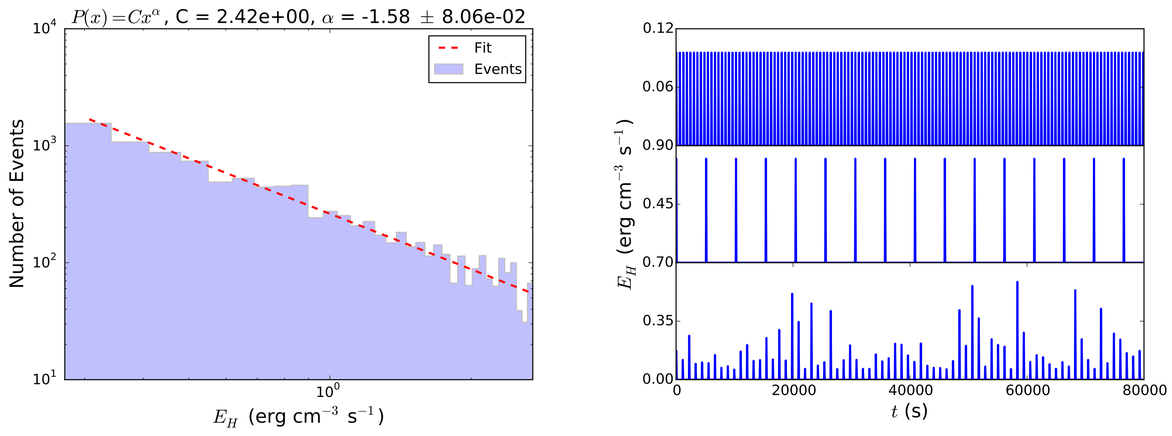

(a) (b)

Figure 2: 2(a) Resulting amplitude distribution for $\alpha = -1.5$, $L = 40$ Mm, $T_N = 5000$ s. For each T_N value, 10^4 events are included such that the power-law distribution is adequately represented. 2(b) Sample heating functions for **top:** uniform amplitudes, $T_N = 500$ s, **middle:** uniform amplitudes, $T_N = 5000$ s, and **bottom:** power-law distributed amplitudes ($\alpha = -1.5$), $T_N = 1000$ s. All events are 100 s in duration. In this study, we have used $250 < T_N < 5000$ s and $\alpha = -1.5, -2.0, -2.5$

Emission Measure Curves

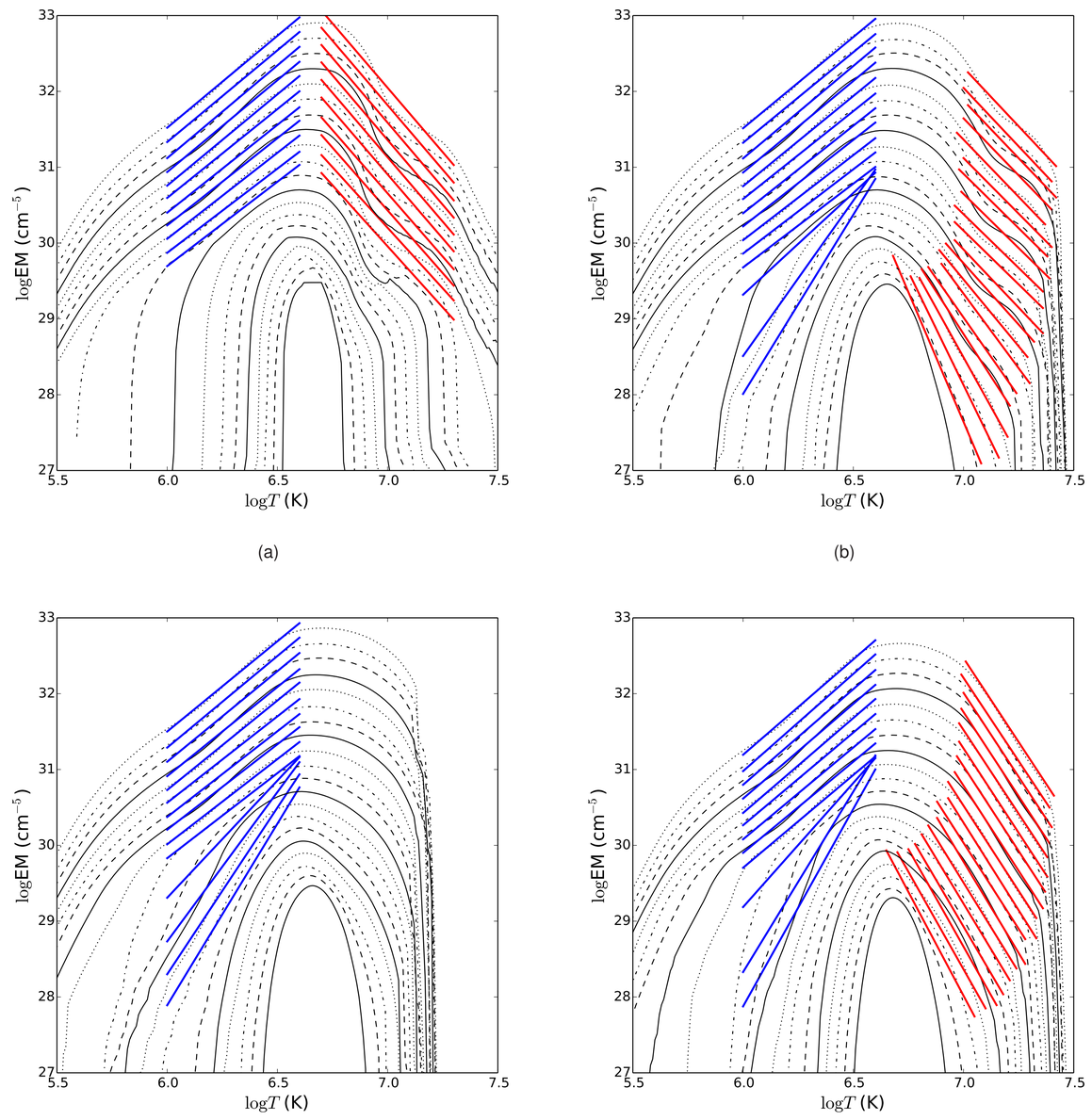

(a) (b) (c) (d)

Figure 3: Emission measure curves constructed in the manner of Cargill [2] using EM $= n^2 L$ and method of Klimchuk et al. [6] for half-length of $L = 40$ Mm using the Raymond-Klimchuk loss function with overlaid hot- and cool-branch fits for 3(a) electron heating, $\alpha =$uniform, 3(b) electron heating, $\alpha = -1.5$, 3(c) ion heating, $\alpha = -1.5$, and 3(d) both species heated equally (single-fluid EBTEL code) and $\alpha = -1.5$. Each curve is separated by an artificial spacing of 0.2 with different curves corresponding to differing values of T_N; bottom curve corresponds to $T_N = 250$ s, the next curve $T_N = 500$ s, and so on up to $T_N = 5000$ s.

Emission Measure Slopes

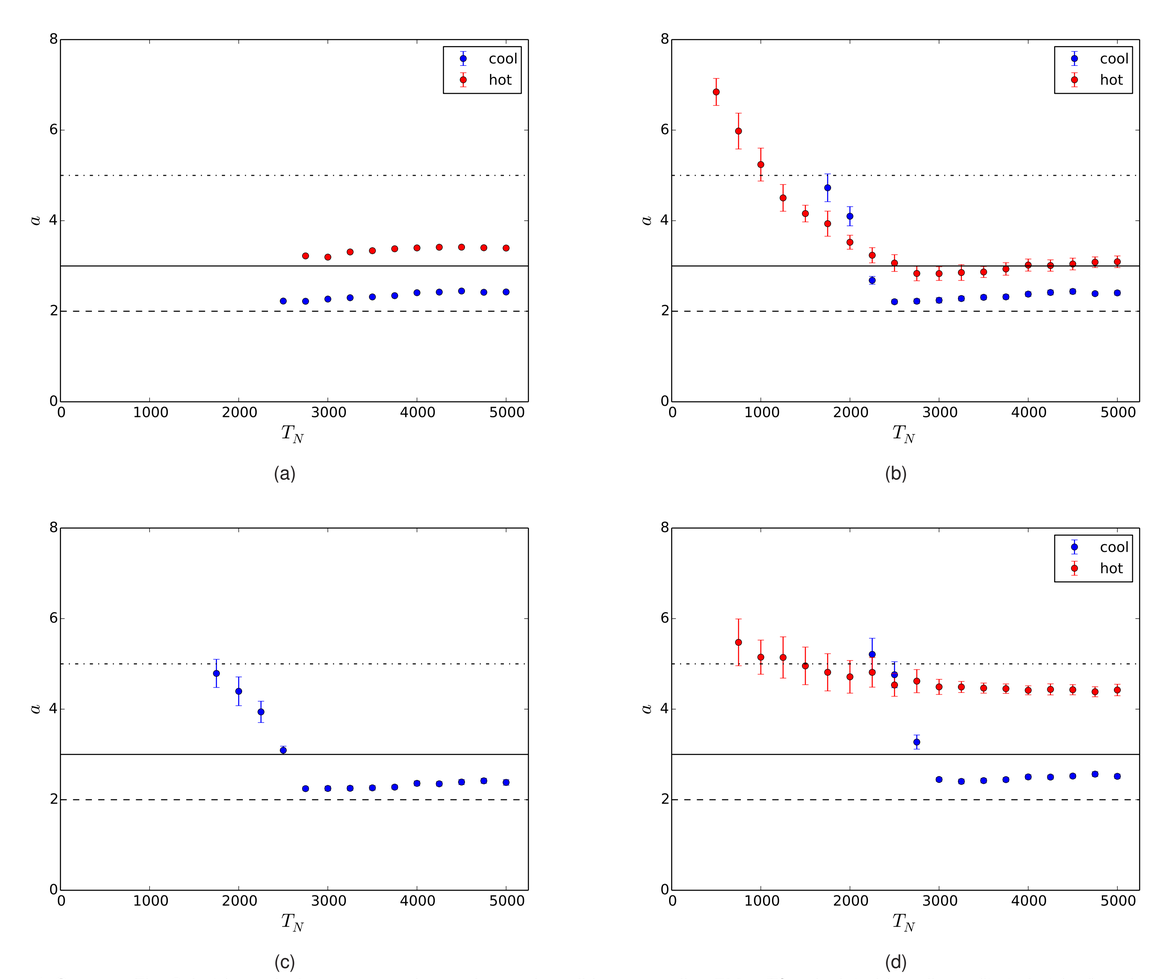

(a) (b) (c) (d)

Figure 4: Same as Fig. 3, but for emission measure slope values, a in well-known scaling EM $\propto T^a$, calculated from linear fits to hot (red) and cool (blue) branches for varying T_N. All cool branches are fit on the interval $6.0 \leq \log(T) \leq 6.6$ while the limits on the hot branches are $6.8 \lesssim \log(T) \lesssim 7.3$ and adjusted such that the fit is always done hotward of the temperature of peak EM with an upper limit placed at roughly where the EM curve begins to drop off sharply. Ion heating EM curves have no hot-shoulder fit because the EM value drops off sharply after the peak. Error bars correspond to 1σ calculated over many runs used to properly sample power-law distribution.

Conclusions

- Pronounced hot shoulder for electron-only heating (uniform and $\alpha = -1.5$) while single-fluid case shows nearly linear hot branch, no visible hot shoulder
- In electron-only heating, no energy partitioned to ions $\rightarrow$ more high-T emission
- Ion-only heating shows sharp drop hotward of peak; T_e never "sees" peak ion temperature because of collisional coupling timescale
- For all cases, $2 \leq a_{\rm cool} \leq 3$ for $T_N \geq 3000$ s, consistent with $2 \lesssim a_{\rm cool} \lesssim 5$ reported in observations and simulations [see Table 3 of 1]
- $3 \lesssim a_{\rm hot} \lesssim 7$ though single-fluid case is only one well-described by linear fit (see Fig. 3(d))
- Future work: improved calculations of EM, DEM through forward modeling and EM-loci or MCMC [5] method; more realistic determination of input-energy budget (i.e $Q \propto T_N, T_N^2$ [2])

References

[1] Bradshaw, S. J., Klimchuk, J. A., & Reep, J. W. 2012, ApJ, 758, 53
[2] Cargill, P. J. 2014, ApJ, 784, 49
[3] Cargill, P. J., Bradshaw, S. J., & Klimchuk, J. A. 2012, ApJ, 752, 161
[4] —. 2012, ApJ, 758, 5
[5] Kashyap, V., & Drake, J. J. 1998, ApJ, 503, 450
[6] Klimchuk, J. A., Patsourakos, S., & Cargill, P. J. 2008, ApJ, 682, 1351
[7] Markovskii, S. A., & Hollweg, J. V. 2004, ApJ, 609, 1112
[8] Parker, E. N. 1988, ApJ, 330, 474
[9] Reep, J. W., Bradshaw, S. J., & Klimchuk, J. A. 2013, ApJ, 764, 193
[10] Warren, H. P., Brooks, D. H., & Winebarger, A. R. 2011, ApJ, 734, 90
[11] Warren, H. P., Winebarger, A. R., & Brooks, D. H. 2012, ApJ, 759, 141

Department of Physics and Astronomy - Rice University - Houston, TX

wtbarnes

Mail: will.t.barnes@rice.edu